Frontiers of Information Technology & Electronic Engineering
www.jzus.zju.edu.cn; engineering.cae.cn; www.springerlink.com
ISSN 2095-9184 (print); ISSN 2095-9230 (online)
E-mail: jzus@zju.edu.cn

Design of a hybrid magnetomotive force electromechanical valve actuator*

Jawad ASLAM[†1,2], Xing-hu LI[1], Faira Kanwal JANJUA[3]

([1]*School of Transportation Science and Engineering, Beihang University, Beijing 100191, China*)

([2]*School of Mechanical and Manufacturing Engineering, National University of Science and Technology, Islamabad 46000, Pakistan*)

([3]*School of Natural Sciences, University of Engineering and Technology, Lahore 54000, Pakistan*)

[†]E-mail: jawad_mtsa@yahoo.com

Received May 6, 2016; Revision accepted Aug. 7, 2016; Crosschecked Oct. 29, 2017

Abstract: We propose a novel axis-symmetric modified hybrid permanent magnet (PM)/electromagnet (EM) magnetomotive force actuator for a variable valve timing camless engine. The design provides a large magnetic force with low energy consumption, low coil inductance, PM demagnetization isolation, and improved transient response. Simulation and experimental results confirm forces of about 200 N (in the presence of coil current) at the equilibrium position and 500 N (in the absence of coil current) at the armature seat. We compared our proposed design with a double solenoid valve actuator (DSVA). The finite element method (FEM) designs of the DSVA and our proposed valve actuator were validated by experiments performed on manufactured prototypes.

Key words: Permanent magnet; Electromagnet; Variable valve timing; Camless engine; Magnetomotive force
https://doi.org/10.1631/FITEE.1601215 **CLC number:** TM351

1 Introduction

Traditional engines use a camshaft for valve timing (intake and exhaust). The camshaft lifts a poppet valve to a fixed displacement and time for a limited operating range. The camshaft lobe can be optimized for a certain engine speed. However, the optimization does not guarantee optimum behavior over a wide range of engine operations (Hara *et al.*, 2009), which results in compromises among engine torque, fuel efficiency, and exhaust emissions. Therefore, original equipment manufacturers (OEMs) have developed and employed variable valve actuation systems to optimize valve timing in response to operating conditions. Variable valve timing (VVT) changes the camshaft phase of the intake valve with respect to the exhaust valve, while variable valve lift (VVL) provides different valve, displacements. VVT control results in a 20% reduction in CO_2 emissions, a 15% improvement in fuel economy, a 10% improvement in torque output, and a 50% reduction in hydrocarbon (HC) emissions at cold start (Sellnau and Rask, 2003; Chladny *et al.*, 2005; Clark *et al.*, 2005; Kim and Lieu, 2005; 2007; Kim and Chang, 2006; Rens *et al.*, 2006; Hara *et al.*, 2009; Kim *et al.*, 2010).

VVT actuators pioneered over the years by OEMs include mechanical, hydraulic, motorized, and electromechanical/electromagnetic actuators. The most common commercial actuators are the Toyota VVT-i, Honda VTEC, Hitachi VEL, Nissan Neo VVL, Mitsubishi MIVEC, and Mazda S-VT (Sellnau and Rask, 2003). The present VVT systems lack continuous timing change, add complexity to the engine,

* Project supported by the State Key Laboratory of Automotive Safety and Energy, Tsinghua University (No. KF14112) and the State Key Laboratory of Engines, Tianjin University (No. K2014-6)

ORCID: Jawad ASLAM http://orcid.org/0000-0002-8151-5457

and above all offer only limited improvement in engine torque (Kim and Lieu, 2005). A linear electromagnetic motor (LEM) based camless engine valve train has been reported (Liu and Chang, 2011a; 2011b; Mercorelli, 2015). The problem with LEMs is their requirement for constant high power to generate a large force during the valve opening operation. LEM structure includes either a moving coil (Liu and Chang, 2011a; 2011b; Liu *et al.*, 2011; Yang *et al.*, 2011) or a magnet (Mercorelli, 2015), which results in a relatively short operational life of the actuator. Rotational motor (RM) based actuators have been proposed and prototyped (Fabbrini *et al.*, 2012; Mercorelli, 2012a; 2012b). An RM requires the design of rotational to linear linkage for pushing the valve open and closed. The high force of an RM needs high current dissipation and accurate linkage design. Studies on camless engine valve trains also included hydraulic electronic valve actuators (HEVAs) (Gillela *et al.*, 2014; Mercorelli *et al.*, 2012). HEVA systems put an added load of a pump on the engine, thereby reducing engine efficiency. Hydraulic fluid performance is affected by temperature and dust. HEVAs are expensive to prototype and hydraulic fluid is flammable, which discourages bulk production. Piezo electric actuated valves add hysteresis to the system and therefore are not applicable for position control (Mercorelli *et al.*, 2012). Recently, fully flexible double solenoid valve actuators (DSVAs) have been prototyped, but none has yet been commercialized due to inherent problems of acoustic noise, high power consumption, complexity, control, and mechanical wear. A DSVA design is shown in Fig. 1.

A harmonically oscillating spring mass system defines the transition time (closing/opening of the valve), which is directly proportional to the spring constant, armature mass, and coefficient of viscous damping. The problem of high power consumption is partly due to the larger coil current input required to overcome the spring force and keep the armature latched at the solenoid. The other contributing factor is the power requirement at start-up to open/close the valve when the armature is at the equilibrium position between the two solenoids (Kim and Lieu, 2007).

Power consumption can be reduced by the use of a hybrid permanent magnet (PM) and electromagnet (EM) valve actuator. The hybrid valve actuator (HVA) reduces power consumption by applying PM

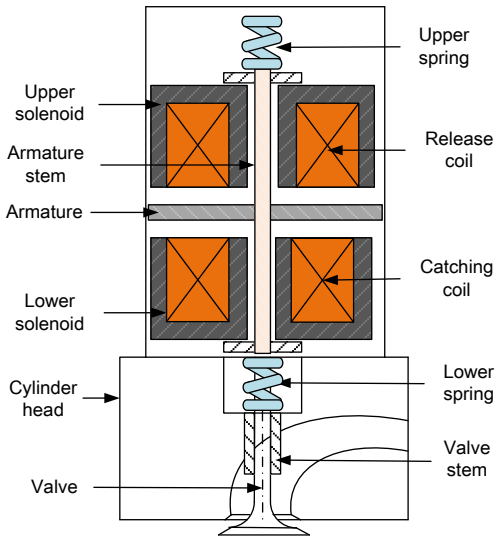

Fig. 1 Double solenoid valve actuator

reluctance to hold the valve open/closed instead of an EM (Rens *et al.*, 2006). Therefore, at start-up the armature is latched; the valve is open or closed and is not in the equilibrium position. An HVA with a rectangular core and a non-asymmetric armature has been studied (Chladny *et al.*, 2005; Clark *et al.*, 2005; Kim and Lieu, 2005; 2007; Kim and Chang, 2006; Rens *et al.*, 2006). A rectangular core HVA requires a linear motion of the armature stem to prevent failure of operation. Mechanical wear prevails due to the absence of cylindrical motion and torsional vibration. The PM flux is in series with the EM coil flux, causing demagnetization of the PM by excessive inverse current. Mechanical wear is limited by employing a symmetric armature (Albert *et al.*, 2009). In an axis-symmetric reluctance HVA, PM flux is oriented parallel to the EM coil flux with parasitic air gaps to avoid demagnetization of the PM (Liu and Chang, 2011a; 2011b; Shiao and Dat, 2013).

In this study, we propose an axis-symmetric, low inductance, and hybrid PM/EM actuator with a novel modified cylindrical core. The modified hybrid valve actuator (MHVA) is optimally designed and simulated in the commercial finite element method (FEM) software ANSYS Maxwell. The performance of MHVA is compared to that of a DSVA with similar construction parameters and design. Results from experiments conducted on manufactured prototypes of DSVA and MHVA are presented to authenticate the FEM analysis.

2 Design of a hybrid valve actuator

An MHVA is composed of two pre-stressed springs, which keep the armature at the equilibrium position between two solenoids (Fig. 2). The spring constant determines the transient time of the spring-mass system. The soft iron yoke is divided into three parts, the yoke, yoke cover plate, and yoke base plate, separated by secondary air gaps. The secondary air gaps provide a detour to the EM coil flux, preventing circulation through the PM causing demagnetization.

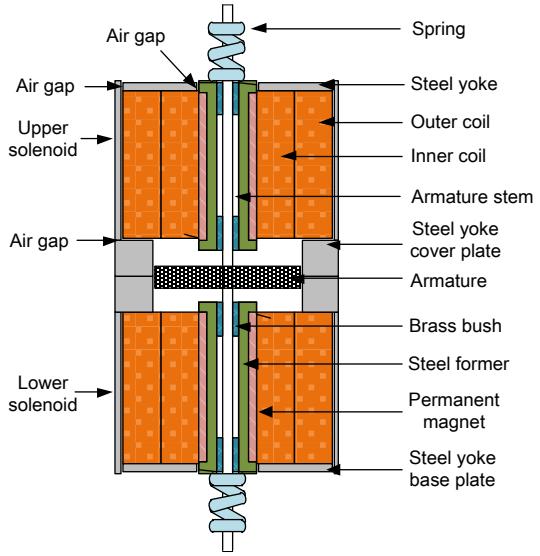

Fig. 2 Structure of the proposed modified hybrid valve actuator (MHVA)

PM flux is oriented parallel to the EM coil flux. The diametric polarized cylindrical PM reluctance latches the armature at the seating position in the absence of coil current. The coil inductance is reduced by introducing two cylindrical parallel coils, thereby reducing the transient time by assisting the swift rise in current (Cope and Wright, 2006; Vu and Pyung, 2013). The coils have a similar number of turns and wire diameter, resulting in low coil resistance for the proposed design.

The operation control of MHVA is depicted in Fig. 3. At the beginning of the cycle the armature is latched to the lower solenoid seat, keeping the valve open (Fig. 3a). Reluctance from the PM generates a holding force (F_H) greater than the spring force (F_S) to open the valve. The coils are recharged with inverse current generating a release flux to reduce the PM flux, thereby assisting the spring force (F_S) in freeing the armature from the lower solenoid seat (Fig. 3b) and running towards the valve closing position. Coils are discharged as the armature is released and crosses the equilibrium position (Fig. 3c). Catching of the armature is assisted by charging coils at the upper solenoid, thereby strengthening the PM reluctance to overcome F_S (Fig. 3d).

The coils are discharged once the armature is latched at the upper solenoid seat and PM reluctance holds the valve closed (Fig. 3e). The process is repeated to open the valve (Figs. 3f–3a). The energy required is decreased as the coil excitation period is reduced by the PM/EM hybrid magnetomotive force that keeps the armature latched at the solenoid seat in the absence of coil current.

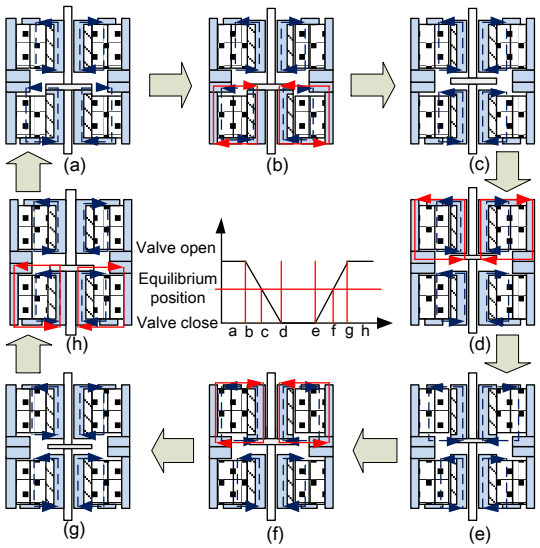

Fig. 3 Working process of a modified hybrid valve actuator (MHVA)

Blue dotted and red lines represent the flux generated by PM and EM, respectively. References to color refer to the online version of this figure

A DSVA requires constant coil charging to hold a valve at the open/closed position. During low engine speeds, the open/closed valve duration is extended, thus increasing power consumption over that period, unlike in an MHVA. At engine startup in an MHVA, the armature is latched at the upper/lower solenoid; therefore, the need for large startup energy is diminished. For an MHVA, variable valve displacement (engine cylinder turned off) is realized without power consumption, which improves fuel economy at low engine speeds.

3 FEM holding force analysis

The MHVA holding force (F_H) depends on the dimensions of the armature, yoke, yoke cover plate, yoke base plate, PM, and air gaps. The dimensions of MHVA are illustrated in Fig. 4. Optimal values of construction parameters were refined by 2D static analysis in ANSYS Maxwell. The proposed design has vertical symmetry, and therefore the solenoid (upper/lower) can be modeled separately to reduce complexity and computational time.

The materials used in FEM analysis and design and their relative permeabilities are listed in Table 1. The nonlinear permeability of steel-1008 selected and used for the armature is depicted in Fig. 5. The optimal construction parameters of MHVA are shown in Table 2. A DSVA has similar parameters except that the PM is replaced by a similarly sized iron cylinder. The F_H static analysis was conducted for MHVA and DSVA for different armature positions using ANSYS Maxwell (Fig. 6).

Table 1 Modified hybrid valve actuator (MHVA) materials and their relative permeabilities

Material	Relative permeability
Copper	0.999 991
Iron	4000
NdFe35	1.044 573

The F_H for MHVA shows increases of 92.3%, 80%, and 64.2% at the armature seat on applications of 500, 1000, and 1500 Ampere-turn (Aturn) current, respectively, in comparison to DSVA for the same charging current. In the absence of a charging current, MHVA generates 500 N of F_H compared with zero for DSVA.

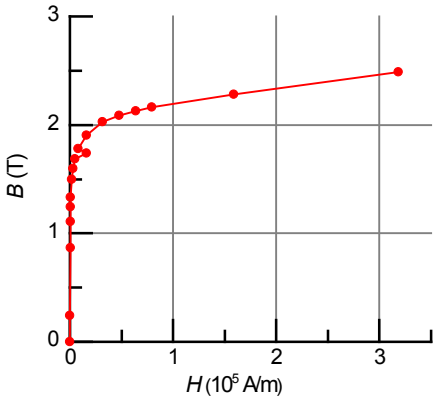

Fig. 5 *B–H* curve of steel-1008

MHVA generates F_H in the absence of a charging current due to PM reluctance, which requires an inverse current excitation to reduce F_H to release the armature from its seat. The inverse current charging effect on F_H at the armature seat is depicted in Fig. 6b. F_H decreases with increasing inverse current amplitude, reaching the minima at a current of 1500 Aturn.

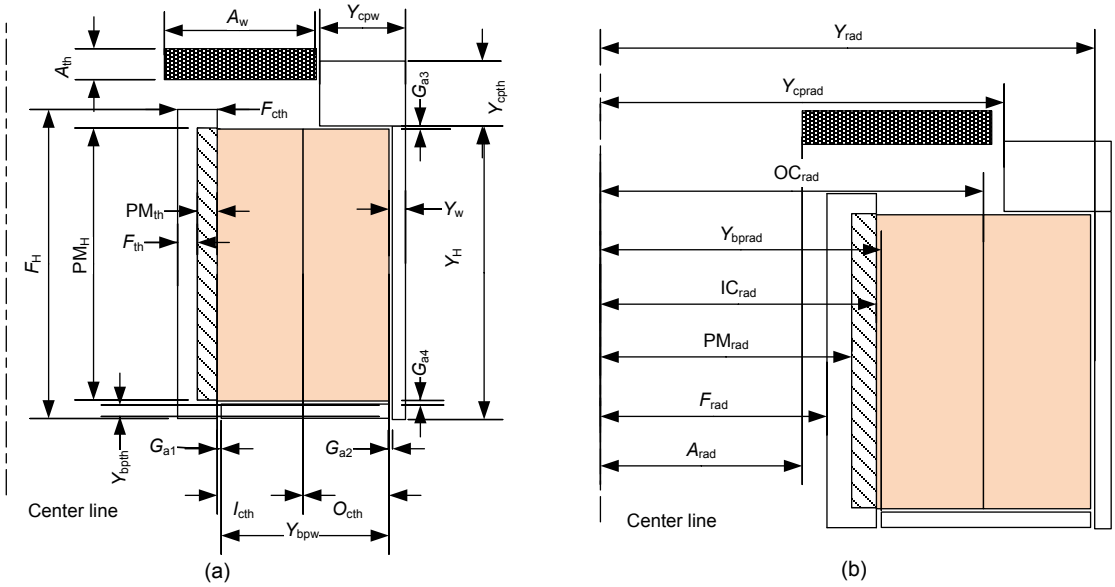

Fig. 4 Construction parameters of a modified hybrid valve actuator (MHVA)
Subscripts denote thickness (th), width (w), radius (rad), height (H), air (a*), plate (p), cover (c), and base (b)

Table 2 Optimal values of critical parameters

Unit	Size notation	Size value (mm×mm×mm)	Material
Armature	$A_{rad}\times A_w\times A_{th}$	3×22×5	Steel-1008
Former	$F_{rad}\times F_H\times F_{cth}\times F_{th}$	8×58×8×4	Iron
Permanent magnet	$P_{Mrad}\times P_{MH}\times P_{Mth}$	8×50×4	NdFe35
Inner coil	$I_{crad}\times I_{cth}$	12×14	Copper
Outer coil	$O_{crad}\times O_{cth}$	26×14	Copper
Yoke cover plate	$Y_{cprad}\times Y_{cpw}\times Y_{cpth}$	27.7×17.5×9	Iron
Yoke	$Y_{rad}\times Y_H\times Y_w$	40.2×55.5×3	Iron
Yoke base plate	$Y_{bprad}\times Y_{bpw}\times Y_{bpth}$	13×27×5	Iron

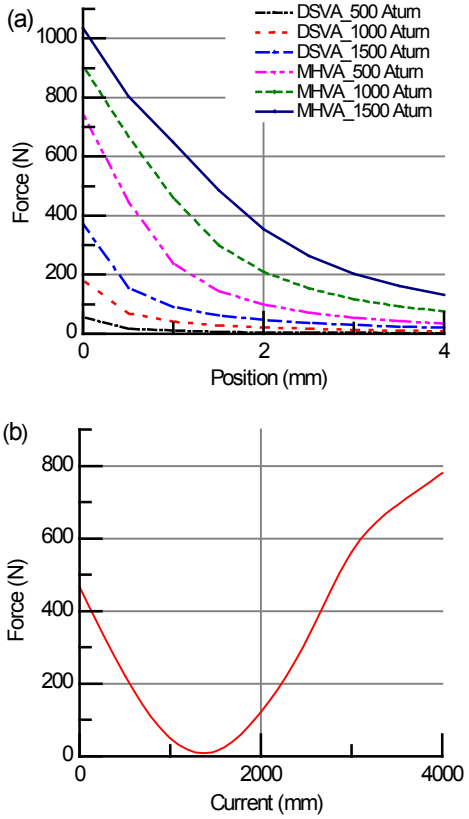

Fig. 6 FEM force analysis at different positions: (a) flux strengthening current for DSVA and MHVA; (b) flux weakening current for MHVA

Further increases in inverse excitation current result in amplification of F_H due to the dominance of EM flux over PM reluctance decrease. The flux density of MHVA is shown in Fig. 7.

For an MHVA in the absence of EM coil excitation, PM reluctance generates F_H to keep the armature latched. The maximum flux passes through the former and armature (Fig. 7a).

Flux concentrates in the armature, the upper region of the former, and the contact area between the

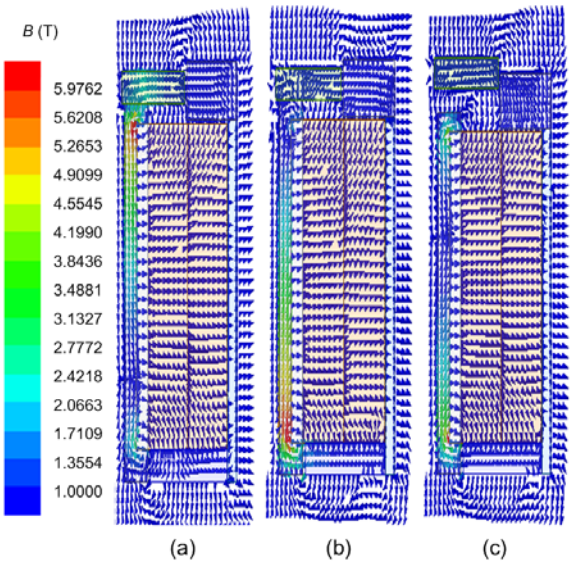

Fig. 7 Flux densities at the seating position without inverse current (a), seating position with inverse current (b), and equilibrium position with no inverse current (c)

two, due to the enlarged metal area. The flux direction and concentration level at the two ends of the former are opposite. The flux orientation in the yoke cover plate and yoke are in a similar direction to that of the armature, thereby assisting in the larger F_H. The yoke base plate houses two different flux orientations at both ends; thus, the magnetic force generated is minimal in the lower region and maximal in the former upper region. The air gap in the area of contact is negligible compared to G_{a1} (between the former and the yoke base plate). Therefore, the flux is concentrated in the armature, contact region at the former, yoke cover plate, and yoke, and partially in the yoke base plate. On excitation of the coils with inverse current, the PM flux is opposed and canceled by the EM flux (Fig. 7b). The flux is concentrated in the lower region of the former; therefore, the concentration and orientation at the two ends are different. The flux orientation at the yoke, yoke cover plate, base plate, and lower end of the former is the same as that generated by the EM. The F_H at the armature is negligible due to the different flux orientation at the ends of the armature and the minimal flux flow. The flux in the yoke base plate has a single orientation as the coils are in contact with the yoke, yoke cover plate, and yoke base plate (Fig. 7b). The armature at the equilibrium position with no coil excitation is shown in Fig. 7c. The air gap between the former and armature

is greater than the secondary air gaps; thus, flux is concentrated in the lower region of the former due to the large metal area. The flux flows through the armature and yoke cover plate, and partially in the yoke in a similar orientation to that in the upper region of the former. Flux in the opposite orientation is observed in the former lower region, yoke lower region, and yoke base plate, leading to minimum F_H.

4 Prototype and testing

Prototypes of DSVA and MHVA were manufactured along with a cold testing rig. The manufactured prototypes had similar structural dimensions except that in DSVA an iron cylinder was substituted for PM. The prototype actuators and rig are shown in Fig. 8. Fig. 8a depicts the manufactured prototype lower solenoid with the armature and armature stem. Fabricated prototype coils were wounded with AWG Wiring Standard sizing chart 15 gauge (1.4 mm) copper wire with 400 turns around a nylon bobbin. The overall resistance of the parallel coils was 0.35 Ω.

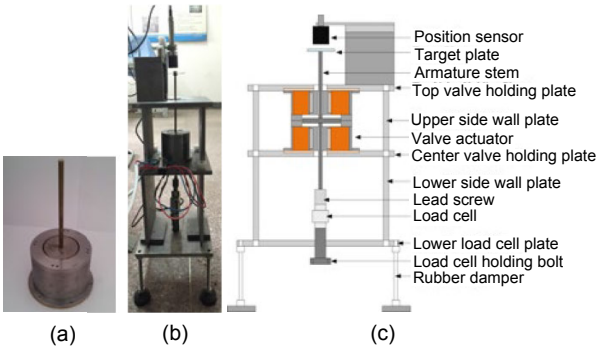

Fig. 8 Manufactured actuator prototype (a), static rig arrangement (b), and dynamic rig arrangement schematic (c)

Static and dynamic tests were performed on the cold testing rig (Figs. 8b and 8c). The rig comprised a center valve holding plate where the lower half of the solenoid valve was bolted. The lower plate held load cell BUFSON sensors BSLZ-1 with a load bearing capacity of 200 kg. The signal of the load cell was amplified by a BUFSON strain gauge amplifier BSFY-1 from 0 to 5 V. The armature position was varied by means of a lead screw at the top of the load cell. Armature displacement was detected by an HZ-891XL eddy current sensor (Shanghai Aerospace Vibration Instruments Co. Ltd., China) mounted at the top of the valve holding plate (Figs. 8b and 8c). The eddy current sensor required a 50 mm metal target plate. During static testing, the armature distance was kept constant and force was measured by a load cell at different excitation currents. The excitation current was applied by a 12 V 40 A power supply, whose pulse width modulation (PWM) can be altered to control the input current amplitude. Current was sensed by an LA-50P Hall effect current sensor (LEM, Switzerland). The MHVA valve was driven by a BTS-7970 H-Bridge circuit (Shenzhen Chipskey Technology Co., Ltd., China). The data acquisition (DAQ) and I/O control was implemented by National Instrument (NI) USB-6351. NI LABVIEW was used to program NI USB-6351. For dynamic testing, the load cell and lead screw were removed from the cold testing rig and linear springs with an average spring constant of 18.82 N/mm were added. The spring stress strain curve under compressive load is shown in Fig. 9. The two springs were preloaded to 75.28 N and the armature equilibrium state was between two solenoids, 4 mm away from the valve seat.

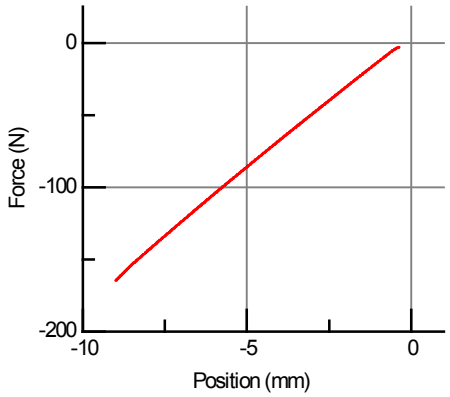

Fig. 9 Spring stress strain curve

Static tests were performed for DSVA and MHVA. The results of static testing of DSVA are depicted in comparison with those of its finite element analysis (FEA) simulation (Fig. 10). A maximum force of 129 N was generated by DSVA at 1500 Aturn current excitation (Fig. 10a). The force error between FEA and experimental values increased as the distance from the armature seating position declined, and excitation current magnitude was amplified (Fig. 10b). A maximum force error of 26.2 N occurred at 1500

Aturn excitation current and 0.5 mm of armature displacement from the valve seat (Fig. 10b). For 1000 Aturn, the error decreased as the armature moved away from the valve seat. At the lower current excitation, the error remained close to zero.

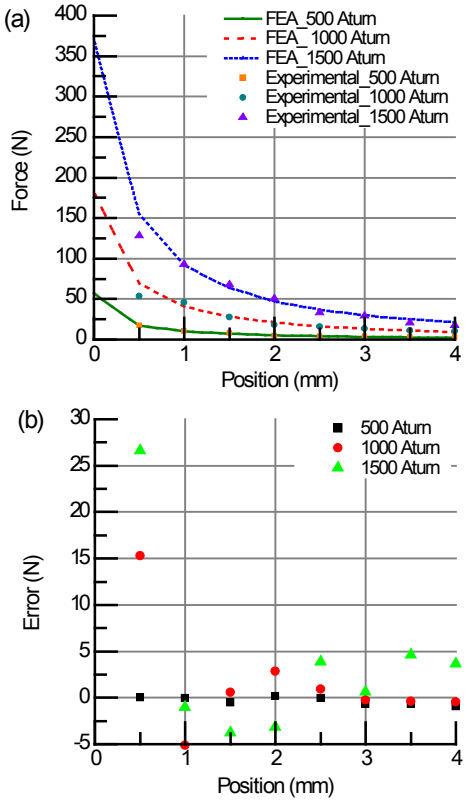

Fig. 10 Static test results for DSVA: (a) force variation with position; (b) force error variation with position

Results of static testing of MHVA are depicted in Fig. 11. The force generated by MHVA decreased experimentally with the decline in armature displacement from the valve seat (Fig. 11a). The force error increased with the increase of current excitation, reaching a maximum of 74.5 N for 1500 Aturn current excitation, when the armature was 0.5 mm away from the valve seat. The force error declined as the armature ascended towards the equilibrium position. The force errors from FEA and experimental results are depicted in Fig. 11b. The force errors for DSVA and MHVA suggest good agreement between experimental and FEA simulation results. The force error occurs due to manufacturing and parameter inaccuracies. The excitation current complementing the PM flux of MHVA showed promising behavior.

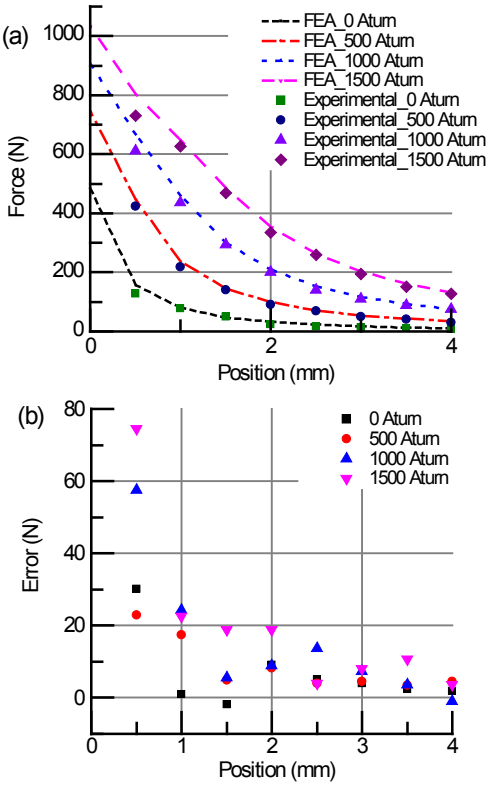

Fig. 11 Static test results for MHVA: (a) force variation with position; (b) force error variation with position

Another studied aspect of the behavior of MHVA was weakening of the PM flux by inverse excitation of the coils. The minimum F_H at the armature seat was produced by 1450 Aturn, as concluded from FEA results. Experimental data showed minima at 1500 Aturn current excitation that reduced F_H to 17.70 N. The F_H reduction at different inverse current excitations is shown in Fig. 12. The reduction in force was slightly less than that predicted by FEA simulation. The experimental data approximately followed the FEA results. Therefore, we deduce from the static behavior experimental results of MHVA and DSVA that the desired performance can be achieved. MHVA had a larger force to volume ratio for the same current compared with DSVA.

The transient time of the armature from the lower to the upper solenoid seat and vice versa is dependent on the time constant of the spring and the mass of the armature assembly (armature, armature stem).

A smaller time constant facilitates system performance. The friction and damping coefficient of the system increase the time constant of the spring and

armature assembly mass system. The dynamic behavior of an armature assembly with a mass of 130 g and an 18.82 N/mm preloaded spring is illustrated in Fig. 13. The transient time for the armature to travel form the upper to the lower solenoid seat is 3 ms, with an open loop landing velocity of 2.01 m/s.

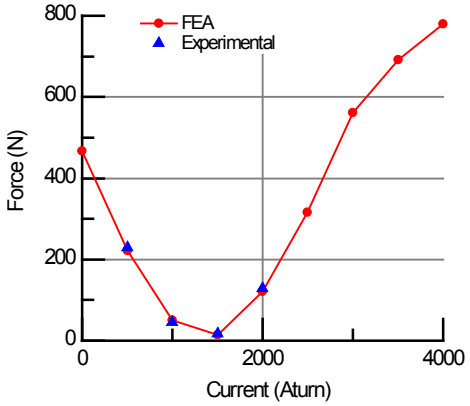

Fig. 12 Inverse current excitation effects on the F_H of MHVA

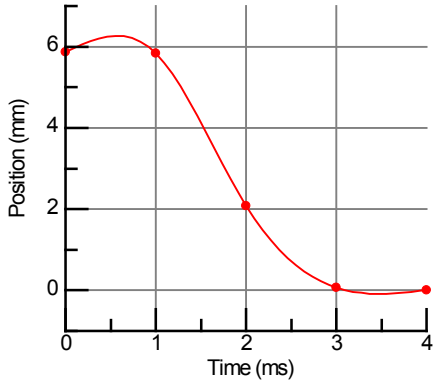

Fig. 13 Dynamic behavior of armature assembly mass and springs

MHVA generates a larger force than DSVA for the same excitation current. An F_H of 500 N is generated at 0 Aturn input current by MHVA, whereas DSVA generates 0 N force. DSVA requires an excitation current to generate F_H force. A maximum force of 370 N is generated at 1500 Aturn coil, which is 75% less than that generated by MHVA at the same excitation. The dynamic behavior of the two is the same, as it depends on the spring mass system formed by the two springs and the armature assembly mass. Therefore, the proposed MHVA performs better that DVSA. MHVA requires inverse current excitation to de-latch the armature. The coils are excited with an inverse current for a smaller period than that required by DSVA to hold the armature latched. For example, at an engine speed of 6000 r/min, the armature is held at the seat for a minimum of 10 ms and inverse excitation lasts 3 ms for MHVA. Thus, DVSA dissipates more power than MHVA.

5 Conclusions

A novel modified hybrid valve actuator is proposed in this study. The valve actuator uses PM/EM reluctance to achieve reduced energy dissipation and generation of a large F_H. MHVA has an improved volume to force ratio with low energy consumption compared to a DSVA of the same constructional parameters. FEM simulations were validated by experimental results. The results can be used to formulate a mathematical model for use in control design to reduce the impact velocity of the armature.

References

Albert, J., Banucu, R., Hafla, W., *et al*., 2009. Simulation based development of a valve actuator for alternative drives using BEM-FEM code. *IEEE Trans. Magn.*, **45**(3): 1744-1747. https://doi.org/10.1109/TMAG.2009.2012804

Chladny, R.R., Koch, C.R., Lynch, A.F., 2005. Modeling automotive gas-exchange solenoid valve actuators. *IEEE Trans. Magn.*, **41**(3):1155-1162. https://doi.org/10.1109/TMAG.2004.841701

Clark, R.E., Jewell, G.W., Forrest, S.J., *et al*., 2005. Design features for enhancing the performance of electromagnetic valve actuation systems. *IEEE Trans. Magn.*, **41**(3): 1163-1168. http://doi.org/10.1109/TMAG.2004.843342

Cope, D., Wright, A., 2006. Electromagnetic Fully Flexible Valve Actuator. SAE Technical Paper No. 2006-01-0044. https://doi.org/10.4271/2006-01-0044

Fabbrini, A., Garolli, A., Mercorelli, P., 2012. A trajectory generation algorithm for optimal consumption in electromagnetic actuators. *IEEE Trans. Contr. Syst. Techn.*, **20**(4):1025-1032. https://doi.org/10.1109/TCST.2011.2159006

Gillela, P.K., Song, X., Cun, Z., 2014. Time varying internal model based control of a camless engine valve actuation system. *IEEE Trans. Contr. Syst. Techn.*, **22**(4):1498-1510. https://doi.org/10.1109/TCST.2013.2280902

Hara, S., Suga, S., Wanatabe, S., *et al*., 2009. Variable valve actuation systems for environmental friendly engines. *Hitachi Rev.*, **58**(7):319-324.

Kim, J., Chang, J., 2006. A new electromagnetic linear actuator for quick latching. 12th Biennial IEEE Conf. on Electromagnetic Field Computation, p.70. https://doi.org/10.1109/CEFC-06.2006.1632862

Kim, J., Lieu, D.K., 2005. Designs for a new, quick-response, latching electromagnetic valve. IEEE Int. Conf. on Electric Machines and Drives, p.1773-1779. https://doi.org/10.1109/IEMDC.2005.195960

Kim, J., Lieu, D.K., 2007. A new electromagentic valve actuator with less energy consumption for variable valve timing. *J. Mech. Sci. Eng.*, **21**(4):602-606. https://doi.org/10.1007/BF03026964

Kim, J., Chang, J.H., Park, S.M., *et al*., 2010. A novel electromagnetic latching device for variable valve timing in automotive engine. 14th Biennial IEEE Conf. on Electromagnetics Field Computation, p.1. https://doi.org/10.1109/CEFC.2010.5481044

Liu, J.J., Lu, P.H., Yang, Y.P., *et al*., 2011. Energy compensation for soft landing control in camless engine with electromagnetic valve actuator. Int. Conf. on Electrical Machines and Systems, p.1-6. https://doi.org/10.1109/ICEMS.2011.6073424

Liu, L., Chang, S., 2011a. Improvement of valve seating performance of engine's electromagnetic valve train. *Mechatronics*, **21**(7):1234-1238. https://doi.org/10.1016/j.mechatronics.2011.08.002

Liu, L., Chang, S., 2011b. Motion control of an electromagnetic valve actuator based on inverse system method. *Proc. IMECHE Part D: J. Autom. Eng.*, **226**(1):85-93. https://doi.org/10.1177/0954407011413033

Mercorelli, P., 2012a. A hysteresis hybrid extended Kalman filter as an observer for sensorless valve control in camless internal combustion engines. *IEEE Trans. Ind. Appl.*, **48**(6):1940-1949. https://doi.org/10.1109/TIA.2012.2226193

Mercorelli, P., 2012b. A two stage augmented extended Kalman filter as an observer for sensorless control in camless external combustion engines. *IEEE Trans. Ind. Electron.*, **59**(11):4236-4247. https://doi.org/10.1109/TIE.2012.2192892

Mercorelli, P., 2015. A two stage sliding mode high gain observer to reduce uncertainties and disturbances effects for sensorless control in automotive applications. *IEEE Trans. Ind. Electron.*, **62**(9):5929-5940. https://doi.org/10.1109/TIE.2015.2450725

Mercorelli, P., Werner, N., Becker, U., *et al*., 2012. A hybrid hydraulic piezo actuator and its control for camless internal combustion engines. 7th Int. Conf. on Integerated Power Electronics Systems, p.1-6.

Rens, J., Richard, E.C., Geraint, W.J., 2006. Static performance of a polarized permanent-magnet reluctance actuator for internal combustion engine valve actuation. *IEEE Trans. Magn.*, **42**(8):2063-2070. https://doi.org/10.1109/TMAG.2006.877269

Sellnau, M., Rask, E., 2003. Two-Step Variable Valve Actuation for Fuel Economy, Emissions, and Performance. SAE Technical Paper No. 2003-01-0029. https://doi.org/10.4271/2003-01-0029

Shiao, Y., Dat, L.V., 2013. A new electromagnetic valve train with PM/EM actuator in SI engines. *Trans. Can. Soc. Mech. Eng.*, **37**(3):787-796.

Vu, D.T., Pyung, H., 2013. A novel of hybrid magnet engine valve actuator using shorted turn for fast initial response. *Int. J. Inform. Electron. Eng.*, **3**(3):250-253. https://doi.org/10.7763/IJIEE.2013.V3.310

Yang, Y.P., Liu, J.J., Lu, P.H., *et al*., 2011. Multifunctional optimal design of an electromagnetic valve actuator with hybrid magnetomotive force for a camless engine. Int. Conf. on Electrical Machines and Systems, p.1-6. https://doi.org/10.1109/ICEMS.2011.6073321